Characterization of Carboxymethyl Cellulose Films Incorporated with Chinese Fir Essential Oil and Their Application to Quality Improvement of Shine Muscat Grape

Luyu Mei [1], Liuxin Shi [1],*, Xiuli Song [1], Su Liu [1], Qiang Cheng [2], Kai Zhu [3] and Rongxia Zhuge [1]

[1]   College of Light Industry & Food Engineering, Nanjing Forestry University, Nanjing 210037, China; meiluyu@njfu.edu.cn (L.M.); songxiuli910412@163.com (X.S.); liusunjfu@163.com (S.L.); zhugrx@hwagain.com (R.Z.)
[2]   College of Forestry, Nanjing Forestry University, Nanjing 200137, China; chengqiang@njfu.edu.cn
[3]   College of Chemical Engineering, Nanjing Forestry University, Nanjing 200137, China; zhukai53@163.com
*   Correspondence: shiliuxin@njfu.edu.cn; Tel.: +86-25-8542-7841

Abstract: In this study, carboxymethyl cellulose (CMC) films containing 1%, 2%, and 3% Chinese fir essential oil (CFEO) were prepared. The mechanical, optical, physical, microstructural, thermal stability and antimicrobial properties of the films were studied. A traditional steam distillation method was applied for CFEO extraction, in which 35 volatile components were identified. The research results showed that the CMC film mixed with 1% CFEO had the highest tensile strength (TS) and elongation at break (EB), whereas the flexibility was decreased under higher concentrations of CFEO. However, the film's degree of transparency under controlled humidity did not decrease with an increase in CFEO concentration; thus, the sensory evaluation was not adversely effect. Furthermore, the thickness and the water solubility (WS) of film increased after the addition of CFEO. The thermogravimetric analysis (TGA) and differential scanning calorimetry (DSC) results indicated that the thermal stability of the CMC-CFEO films improved. Moreover, the composite films showed excellent inhibitory effects toward Gram-positive bacterias and *Penicillium citrinum*. The treatments of grapes with CMC + 1% CFEO resulted in the best properties during storage. CMC-CFEO film can be a candidate for food packaging due to its excellent performances.

Keywords: food packaging; film; carboxymethyl cellulose; Chinese fir essential oil; grapes

1. Introduction

Owing to the growing importance of food preservation, the methods used for achieving safe food storage have increased significantly in variety. For example, use of a suitable material for food packaging can decrease the food's deterioration rate, thereby extending its shelf life [1]. Active food packaging is a novel concept, meaning that it can extend the shelf life of food through the interaction between the environment provided by packaging materials and the product during the packaging process [2]. One of the most promising approaches is antimicrobial packaging, which inhibits the growth of microorganisms on food surfaces by releasing antimicrobial components. Food packaging material creates a low O_2 and high CO_2 gas environment between the external conditions and the food by forming a film on the surface of food, thereby reducing the exchange rate of the gas or substances used to extend the shelf life. Biodegradable packaging is a new material that replaces synthetic polymers with biopolymers to protect the environment [3]. This biopolymer-based packaging is derived from natural and renewable agricultural and marine sources [1] such as chitosan, starches, and carboxymethyl cellulose (CMC).

Derived from cellulose, CMC polysaccharide is an important agricultural product considered to be safe for human consumption [4]. CMC is widely applied in industries such as food, cosmetics, and pharmaceuticals [5]. In addition, CMC has excellent biodegradability and hydrophilic properties as well as the ability to form transparent films [6,7].

Several studies have shown that the addition of CMC to composite film significantly improves some of film's properties [8,9]. Moreover, CMC has shown strong performance as a desirable matrix to form edible films. Perishable food products need to be protected during their preparation, storage, and distribution to extend their shelf lives [10]. Because of long-term exposure to air, the food surface is easily infested with microorganisms that accelerate deterioration of the food. To solve this problem, CMC can be combined with an antimicrobial agent. Considering the consumer demand for natural and healthy products, essential oils have shown promise for this application.

In recent years, a novel cultivated grape variety has gradually entered the public eye-"Shine Muscat" grape, which was originated in Japan [11]. Shine Muscat is breeded by crossing Akitsu-21 (*Vitis labruscana Baily* × *V. vinifera*) and "Hakunan" (*V. vinifera*) [12]. The pericarp of Shine Muscat grapes is green and has a sweeter taste and they have a longer storage time compared with other grape varieties. They have thin skin and are seedless, so they can be eaten without peeling [13,14]. Therefore, it has been favored by consumers since it was first introduced into the Chinese market. Due to the limited planting area of Shine Muscat grapes in China, long-distance transportation is required, and the price is relatively high compared to similar products. Water loss [15], mechanical injury [16] and fungal decay [17] of fruits are common conditions during transportation. The well-known long-distance storage methods are low-temperature storage, inflatable bag anti-collision packaging and spraying of chemical preservatives. The treatment methods of postharvest grapes include physical methods, such as UV irradiation and sonication; biological methods, such as using yeast species to inhibit *B. cinerea* [18]. Moreover, the coatings were prepared from natural polymers can protect grapes [19,20]. In various studies, SO_2 synthetic fungicide can also preserve grapes, but the residues of chemical preservatives can harm human health [21], so the development of sustainable safe preservatives has become the mainstream of research.

Essential oils are volatile, natural products that are widely used for bacteriostatic, medicinal, and antiseptic purposes as well as for food preservation [22]. These natural, antimicrobial agents are extracted from plants and are composed of numerous chemical compounds [3]. As natural food preservatives, some essential oils can be added to edible film to prevent the growth of microorganisms [23]. Moreover, several studies suggest that essential oils can be combined with CMC to extend the shelf life of fruit and to improve the product's antimicrobial properties [24–26].

Cunninghamia lanceolata, or Chinese fir, is widely planted in southern China [27,28] and plays an important role the country's timber industry [29]. However, the sawdust produced from Chinese fir is usually abandoned or burned, which does not make use of its benefits [28]. To utilize this resource, essential oil can be extracted before this wood byproduct is discarded. Several studies have shown that Chinese fir essential oil (CFEO) has numerous biological effects including antibacterial, antifungal, anti-mite, and anti-mosquito properties [30,31]. In particular, its excellent antibacterial and antifungal properties give CFEO potential as a natural food preservative.

To our knowledge, no study has been conducted thus far on food preservation using CFEO. Therefore, the objectives of this study are to investigate the properties of edible film by combining various concentrations of CFEO with CMC and to evaluate the feasibility of CMC-CFEO edible film by analyzing its characteristics. In addition, the antimicrobial activity of this edible film is studied. This work is of great significance because it is the first to provide a theoretical basis for food preservation using CFEO.

2. Materials and Methods

2.1. Materials

The sawdust of Chinese fir used in this study was produced in Anhui Province (China). The CMC was purchased from Sinopharm Chemical Reagent Co., Ltd. (Shanghai, China) and Tween 80 and glycerol were purchased from Shanghai Macklin Biochemical Co., Ltd. (Shanghai, China). *Staphylococcus aureus* (ATCC6538), *Penicillium citrinum* (ATCC1109),

Escherichia coli (ATCC25922), and *Bacillus subtilis* (ATCC6633) were obtained from Shanghai Luwei Bio-Technology Co. Ltd. (Shanghai, China). Lysogeny broth (LB) and potato dextrose agar (PDA) bouillon were prepared at the Biological Laboratory, Nanjing Forestry University (Nanjing, China). Shine Muscat grapes were purchased from the Yunnan Shine Muscat grapes planting base (Yunnan, China).

2.2. Chinese Fir Essential Oil Extraction

The CFEO was extracted by steam distillation. In this process, 105 g of Chinese fir sawdust with a moisture content of 99.8% was put in a two-necked flask similar to a breathable partition. Subsequently, 600 mL of distilled water was placed in a different flask. Both flasks were interlinked up and down and heated at 100 °C for 4 h of extraction until no more essential oil could be obtained. After volatilization, the CFEO product was collected by adding about 5 mL ether. The remaining solution was CFEO after the ether evaporated by using rotary evaporators at 40 °C. All of the data were confirmed by a preliminary experiment.

2.3. Preparation of Films

The films were prepared as described by Dashipour et al. with some modification [25]. The CMC solution was prepared by dissolving 1 g CMC in 100 mL distilled water (1% *w/v*) under constant magnetic stirring at 70 °C for 40 min until it was complete dissolution was achieved. Afterward, 0.5 mL glycerol (0.5% *w/v* based on the CMC) was added, and the mixture was stirred continuously for 10 min. After cooling, the formed dispersion was cast in glass plates of about 64 cm^2 in area for subsequent use as control film. In addition, CFEO as an antimicrobial agent was added to the CMC solution to obtain final concentrations of 1%, 2%, and 3% (*v/v*). Tween 80 was added to the CFEO at a ratio of 1:10, respectively, and the mixture stirred for 30 min. Afterward, an ultrasound machine (GBP-USC201L, CSIC715, Zhejiang, China) was used at 750 W for 5 min to create uniform mixtures. The blended emulsion was prepared.

Subsequently, the steps for preparing the edible films were described below. These solutions were then cast in the plates after air bubbles were removed. All of the films were dried at 35 °C for about 24 h and were then stored in a desiccator at 25 °C and 55% relative humidity (RH) for preservation.

2.4. Gas Chromatography–Mass Spectrometry Analysis Conditions

The composition was analyzed by using a gas chromatograph–mass spectrometer (GC-MS; ISQ, Thermo-Scientific, Waltham, MA, USA) equipped with a DB-5ms column. Helium was used as a carrier gas at 0.6 mL/min. The oven temperature was kept at 80 °C for 3 min; afterward, the temperature was increased to 280 °C at a rate of 15 °C/min and was kept constant for 3 min. The injection volume was 0.2 μL, and the injector and transfer line temperatures were 250 and 280 °C, respectively. For the MS conditions, the electron impact (EI) ion source temperature was 230 °C; the quadrupole temperature was 150 °C; the EI+ mode was 70 eV; and the mass scan range was 33–450 u.

2.5. Physical Properties of Prepared Films

The film thickness was measured by using a thickness meter (J-DHY03A, Changjiang Paper Instrument Co., Ltd., Sichuan, China) with 0.001 mm sensitivity. The results were obtained by selecting the average of at least five random locations for each film [32].

The water solubility (WS) was determined following the method of Rincon [33]. The films were placed into an oven at 110 °C to obtain the original constant weight (W_0) and were then immersed in 50 mL distilled water for 6 h at room temperature under constant magnetic stirring. Finally, the insoluble films were filtered and dried in an oven to obtain the final constant weight (W_f). The following formula was used to calculate the WS:

$$\text{WS (\%)} = \frac{W_0 - W_f}{W_0} \times 100 \tag{1}$$

2.6. Color Properties of Prepared Films

The lightness (L^*), red/green coordinate (a^*), and yellow/blue coordinate (b^*) color parameters were obtained by using a white colorimeter (ZB-A, Paper State Automation Co., Ltd., Hangzhou, China). A white standard plate was used as the background ($L = 73.04$, $a = -2.00$, $b = 2.61$). The film was removed from the desiccator, and at least three areas were selected for at least three measurements each. The following formula was used to calculate the total color difference (ΔE):

$$\Delta E = \sqrt{(\Delta L)^2 + (\Delta a)^2 + (\Delta b)^2} \tag{2}$$

where $\Delta L = (L^* - L)$; $\Delta a = (a^* - a)$; $\Delta b = (b^* - b)$; L, a, and b are standard plate color parameter values; and L^*, a^*, b^* are film color parameter values.

2.7. Characterization of Prepared Films

The functional groups of the films were determined by Fourier transform infrared spectrometry (FTIR; VERTEX 80 V, Bruker, Ettlingen, Germany). The films were placed on attenuated total reflection (ATR) crystal material to absorb light directly for use with an ATR system. No sample was used for the test background. In total, 16 samples were scanned at a resolution of 4 cm^{-1} in a wavenumber range of 4000–500 cm^{-1}.

The properties of thermal stability were identified by using a thermogravimetric analyzer (TGA; 209 F1, Netzsch, Selb, Germany). The temperature was increased from 25 to 700 °C at a constant rate of 25 °C/min, and N$_2$ gas at a flow rate of 20 mL/min was used as protective gas.

The thermal parameters were measured by differential scanning calorimetry (DSC; 214, Netzsch, Selb, Germany). 6 mg of film pieces were put in a standard aluminum pan. The temperature was increased from 50 to 400 °C at a constant rate of 10 °C/min. The following formula was used to calculate the crystallinity index (Xc):

$$\text{Xc (\%)} = \frac{\Delta Hm}{\Delta Ho} \times 100 \tag{3}$$

where ΔHm is the fusion enthalpy of the blended films, ΔHo is the fusion enthalpy of CMC film. The morphologies of the films were observed by environmental scanning electron microscopy (ESEM; Quanta 200, FEI, Hillsboro, OR, USA) at an accelerating voltage of 20 kV.

2.8. Mechanical Properties of Prepared Films

A universal tensile tester (SANS, MTS Co., Ltd., Minneapolis, MN, USA) was employed to measure the mechanical properties of the films, including the tensile strength (TS), elongation at break (EB) and elastic modulus (EM). Following the Plastics-Determination of Tensile Properties of Films test method (GB13022-1991), all the films were cut to dimensions of 10 cm in length × 1 cm in width. The two ends of the film strips were fixed to the tension machine with an initial separation of 40 mm, and the cross-head speed was 10 mm/min. It is worth noting that all of the film strips were previously equilibrated at conditions of about 50% RH and 25 °C for two days:

$$\text{TS (MPa)} = \frac{F_{max}}{A} \tag{4}$$

$$\text{EB (\%)} = \frac{\Delta L}{L} \times 100 \tag{5}$$

where F_{max} is the maximum tensile force when the film breaks, A is the cross-sectional area of the film, ΔL is the amount of change in film length when stretched, L is the original length of the film.

2.9. Antimicrobial Effects of CFEO and Films

The antimicrobial effects were tested by applying disc diffusion following the method of Poaty with some modification [34]. Specifically, the bacteria and fungus suspensions were mixed with LB agar and PDA media, respectively, at about 55 °C, and each mixture was poured into a Petri dish (d = 90 mm). After solidification, filter paper discs (d = 6 mm) impregnated with the sample were placed on the surface of the agar medium. The plates were incubated at temperatures of 37 and 28 °C for culturing the bacteria and fungi, respectively, for 24 or 48 h in the appropriate incubation chamber. The antimicrobial activities were evaluated by comparing the diameters of the inhibition zones.

2.10. Characterization of Shine Muscat Grape

The blended CMC-CFEO emulsion was coated on plastic wrap (10 cm × 10 cm) and air dried, forming a thin film on the surface. It was wrapped on Shine Muscat grapes, and then the fruits were stored at 25 °C and 40%–60% RH. Each treatment group was replicated five times.

The grapes were weighed with an analytical balance (BSA123S, Satorius Scientific Instruments Co., LTD, Beijing, China) and the weight was recorded every three days. There were 5 grapes in each group and the average value was calculated. The following formula was used to calculate the weight loss rate:

$$\text{Weight loss } (\%) \ = \ \frac{m_0 \ - \ m_f}{m_0} \times 100 \tag{6}$$

where m_0 was initial weight; m_f was final weight.

Each group selected 10 grapes of uniform size and observed the rot on the surface of the grapes every day. The following formula was used to calculate the decay percentage:

$$\text{Decay percentage } (\%) \ = \ \frac{n_r}{n_0} \times 100 \tag{7}$$

where n_r was the number of decayed fruits; n_0 was the number of total fruits.

2.11. Statistical Analysis

IBM SPSS software (version 26, SPSS Inc., Chicago, IL, USA) was used for all experimental data analysis. In addition, one-factor analysis of variance was performed on the experimental data. The measurement results were tested at least three times, all of which were shown as the mean value ± standard error. A p-value < 0.05 indicated a significant difference.

3. Results and Discussion

3.1. Chemical Composition of CFEO

The CFEO composition was analyzed by GC-MS. In total, 35 volatile components were identified and their chemical formulas and area percentages are given in Table 1.

As shown in Table 1, the 35 compounds accounted for 85.73% of the total detected constituents. The volatile components were classified into five main categories, including terpenoids (59.79%), terpenes (24.24%), acids (0.89%), hydrocarbons (0.64%), and proteins (0.17%). Further analysis indicated that the terpenes included mainly sesquiterpenes and a small amount of diterpenes. In addition, the terpenoids included alcohols, esters, and ethers. In particular, the number of species in the ingredients were sixteen terpenes, thirteen alcohols, two esters, two hydrocarbons, one acid, one protein, and one ether. Good bacteriostatic activity was reflected by the terpenoids [23].

The specific ingredients greater than 1% of the CFEO included cedrol (32.69%), α-cedrene (9.53%), sclareol (7.99%), epi-cedrol (3.56%), 13-epimanool (3.35%), cedryl acetate (3.35%), δ-cadinene (2.94%), α-curcumene (2.64%), α-alaskene (2.55%), γ-gurjunene (1.93%), α-bisabolol (1.62%), α-cadinol (1.48%), cadinenol (1.32%), and cubebene (1.21%). The rela-

tively high amount of cedrol is consistent with the results of several previous studies [35–37]. The surveys of some reports suggested that cedrol has potent anti-termite and antimicrobial effects [35,38]. It should be noted that the content of some ingredients differed slightly from that described in previous research [30], which could be attributed to plant origin and variety.

Table 1. Chemical composition of CFEO.

No	Compounds	Chemical Formula	Area%
1	Thujopsene	$C_{15}H_{24}$	0.74
2	α-Caryophyllene	$C_{15}H_{24}$	0.2
3	Germacrene D	$C_{15}H_{24}$	0.46
4	β-Selinene	$C_{15}H_{24}$	0.79
5	γ-Gurjunene	$C_{15}H_{24}$	1.93
6	α-Alaskene	$C_{15}H_{24}$	2.55
7	δ-Cadinene	$C_{15}H_{24}$	2.94
8	α-Cubebene	$C_{15}H_{24}$	0.29
9	α-Calacorene	$C_{15}H_{20}$	0.22
10	Epi-cedrol	$C_{15}H_{26}O$	3.56
11	Cedrol	$C_{15}H_{26}O$	32.69
12	α-Acorenol	$C_{15}H_{26}O$	0.78
13	Cedryl acetate	$C_{17}H_{28}O_2$	3.35
14	Diacetone Alcohol	$C_6H_{12}O_2$	0.13
15	Terpinyl acetate	$C_{12}H_{20}O_2$	0.71
16	α-Cedrene	$C_{15}H_{24}$	9.53
17	α-Curcumene	$C_{15}H_{22}$	2.64
18	Nerolidol	$C_{15}H_{26}O$	0.57
19	T-Cadinenol	$C_{15}H_{26}O$	1.32
20	α-Cadinol	$C_{15}H_{26}O$	1.48
21	α-Bisabolol	$C_{15}H_{26}O$	1.62
22	13-Epimanool	$C_{20}H_{34}O$	3.35
23	H-Cys-Gly-OH	$C_5H_{10}N_2O_3S$	0.17
24	α-Terpineol	$C_{10}H_{18}O$	0.58
25	(*E*)-β-Farnesene	$C_{15}H_{24}$	0.97
26	Germacrene D	$C_{15}H_{24}$	0.46
27	Cubebene	$C_{15}H_{26}O$	1.21
28	Phytane	$C_{20}H_{42}$	0.42
29	β-Caryophyllene	$C_{15}H_{24}$	0.25
30	Palmitic acid	$C_{16}H_{32}O_2$	0.89
31	Cembrene	$C_{20}H_{32}$	0.27
32	Manoyl oxide	$C_{20}H_{34}O$	0.13
33	Sclareol	$C_{20}H_{36}O_2$	7.99
34	Isocembrol	$C_{15}H_{24}O$	0.32
35	*trans*-Squalene	$C_{30}H_{50}$	0.22

3.2. Physical Properties

Table 2 shows the physical property data. The incorporation of the various concentrations of CFEO significantly affected the physical properties of the films. With an increase of CFEO concentration, the thickness of the film gradually increased from 0.095 to 0.195 mm as the film matrix began to be occupied by small molecules of CFEO microdroplets [33]. In previous research, the difference in thickness depended on the concentration of the material and the pouring rate on the surface [25,32,33].

Table 2. Mechanical and physical properties of CMC and blended CMC-CFEO films.

Film	Thickness (mm)	Water Solubility (%)	Tensile Strength (MPa)	Elastic Modulus (MPa)	Elongation at Break (%)
CMC	0.095 ± 0.015 [c]	88.90 ± 0.15 [d]	1.75 ± 0.12 [a]	3.96 ± 0.44 [b]	54.90 ± 0.44 [b]
CMC + 1% CFEO	0.136 ± 0.027 [b]	89.87 ± 0.19 [c]	5.25 ± 2.84 [a]	12.83 ± 1.50 [a]	63.16 ± 1.47 [a]
CMC + 2% CFEO	0.168 ± 0.031 [a]	97.34 ± 0.12 [a]	4.52 ± 2.20 [a]	18.06 ± 1.56 [a]	22.65 ± 2.80 [d]
CMC + 3% CFEO	0.195 ± 0.038 [a]	93.12 ± 0.13 [b]	2.56 ± 0.28 [a]	7.44 ± 1.98 [b]	36.81 ± 2.68 [c]

The letters after the numbers in the same column are not the same, indicating that there is a significant ($p < 0.05$) difference.

The changes in water solubility are also shown in the Table 2. As the concentration of CFEO increased, the film solubility in water also increased. It was related to discontinuity of the polymer matrix. Although essential oils are inherently insoluble in water, adding CMC changed this behavior. CFEO can cause interactions with the polymeric matrix to change their original properties with the concentration of CFEO. In particular, CMC is hydrophilic because it contains a large number of hydroxyl groups, and the substituents break some of the hydrogen bonds. The behavior of the CMC demonstrated its practicality as a film matrix because it promoted excellent dissolution of the essential oil in water. In addition, the degradable nature of the films enable their application in food packaging.

3.3. Color Values Analysis

The color of edible packaging materials is also a major concern of consumers [39]. The "*L*" value brightness criterion ranges from of 0 for darkness to 100 for brightness. Moreover, the "*a*" value represents the range from red (+) to green (-), and the "*b*" value represents that from yellow (+) to blue (-). Table 3 shows that the "*L*" value increased with an increase in CFEO concentration, which indicates that the brightness of the film also increased. However, the "*a*" value decreased to negative with an increase in CFEO. When the CFEO concentration was 1%, the "*a*" value was close to that of the control film. When the concentration increased to 2%, however, the "*a*" value showed an obvious decrease, which differed significantly from that of the control film. This result indicates that the concentration of CFEO is the main factor affecting the "*a*" value. The addition of CFEO led to a steady increase in the "*b*" value, which was significantly different from that of the control film. Because the "*b*" value is related to the yellowish-brown color of CFEO itself, the film color turned yellow to some extent, and the "*b*" tended to increase to positive values. The values "*a*" and "*b*" demonstrated that the color of the CMC-CFEO films became greenish or yellowish compared with that of the control film. The Δ*E* value, as an indicator of the total color difference changes, increased with the concentration of CFEO. The Δ*E* value of film including 1% CFEO was low (Δ*E* ≤ 5), demonstrating that the color difference was not obvious by an observer. When the CFEO concentration was 2% and 3%, the Δ*E* value was 7.8168 and 9.7468, respectively (Δ*E* > 5). It proved that the color difference of the film can be seen by visual inspection.

**Table 3.** Color values of CMC and blended CMC-CFEO films.

Film	*L* *	*a* *	*b* *	Δ*E*
CMC	72.84 ± 0.03 [d]	−3.11 ± 0.10 [a]	4.15 ± 0.09 [d]	1.9066 [d]
CMC + 1% CFEO	77.07 ± 0.03 [c]	−3.51 ± 0.02 [a]	5.16 ± 0.04 [c]	5.0023 [c]
CMC + 2% CFEO	79.04 ± 0.04 [b]	−6.20 ± 0.08 [b]	5.35 ± 0.03 [b]	7.8168 [b]
CMC + 3% CFEO	80.94 ± 0.05 [a]	−6.85 ± 0.01 [c]	5.63 ± 0.03 [a]	9.7468 [a]

The letters after the numbers in the same column are not the same, indicating that there is a significant ($p < 0.05$) difference.

In the macroscopic images of the films shown in Figure 1, the transparency of the film with CFEO decreased relative to that of the pure form. In particular, an increase in CFEO concentration resulted in increasingly lower film transparency. This result is attributed

to light scattering caused by the distribution of the lipid droplets throughout the film network, as opposed to the continuous phase refractive index, and to the volume fraction and concentration of the lipid phase in the emulsion [40,41]. Low film transparency has been shown to postpone the lipid oxidation of food [42].
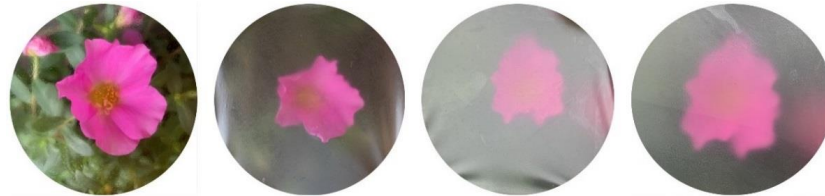
Figure 1. Macroscopic photographs of the films (90% RH) including, from left to right, CMC, CMC + 1% CFEO, CMC + 2% CFEO, and CMC + 3% CFEO.

Moreover, humidity was also found to affect the transparency of the films containing CFEO. As the humidity increased, the transparency of the film containing CFEO steadily decreased. Figures 1 and 2 show photographs captured in an outdoor environment with RH values of about 90% and 40%, respectively. A comparison of the two figures reveals a clear distinction owing to the innate property of Tween-80 as an emulsion and the hygroscopic nature of CMC [43].

Figure 2. Photographs of films at about 50% RH.

3.4. FTIR Analysis

Figure 3 shows the absorption peaks of the films with specific characteristic peaks indicated. The stretching vibration of the functional group –OH is reflected in the absorption peak of wavelength 3289 cm^{-1}, which is attributed mainly to CMC [44]. The band at 2931 cm^{-1} represents the saturated C–H stretching of –CH$_3$. Antisymmetric vibrations of the COO– groups are evident in the peak at 1592 cm^{-1} [33]. The bands at 1413 and 1320 cm^{-1} in the enlarged image on the right are attributed to the bending vibrations of –CH$_2$ or –CH$_3$ and those of –OH, respectively [45]. The band range of 1000–1300 cm^{-1} represents C–O stretching vibration, specifically at the 1104 and 1033 cm^{-1} bands.
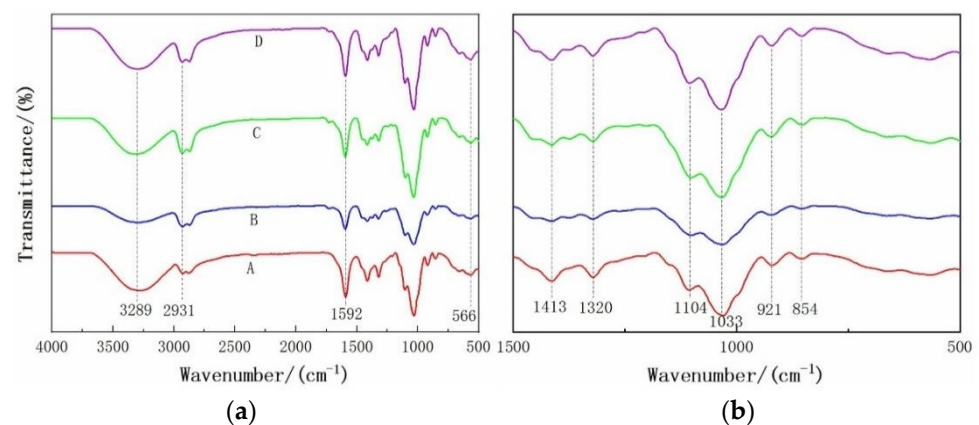

Figure 3. Results of FTIR analysis showing ATR infrared spectroscopy measurement (**a**) and an enlarged view of the same section (**b**) with wavenumbers of 1500–500 cm^{-1}. A: Control film (CMC); B: CMC + 1% CFEO film; C: CMC + 2% CFEO film; D: CMC + 3% CFEO film.

Moreover, a comparison of the four spectra in the figure revealed similar results among the absorption peak points. In the wavelengths of 1500–1000 cm^{-1}, no significant fluctuation occurred among these points owing to the physical incorporation of the added CFEO and CMC. In addition, the spectra of films containing CFEO showed no relationship with the concentration, indicating that CFEO can be effectively combined with CMC [33].

3.5. Thermal Stability Analysis

Thermogravimetric Analysis (TGA) is a vital index for evaluating the thermal stability of materials. Figure 4 shows the TGA and derivative thermogravimetric (DTG) curves of CFEO, CMC film, and blended CMC-CFEO film. The mass loss of CFEO occurred evidently between 100 and 240 °C. While the weight loss of the CMC film occurred twice, the DTG curve for CMC was roughly four processes. The first mass loss occurred between 20 and 130 °C, in which the mass loss was about 5% owing to moisture loss [43], and a second decomposition step was obvious at about 180 °C. The third decomposition step was at 250–330 °C. The two-step decomposition process was partially overlapped. As indicated by the DTG curve, the peak at 270 °C was the temperature where the highest rate of mass loss was attained, declining rapidly to 64% in the temperature range of 180–350 °C owing to the decomposition of methylcellulose and the loss of CO_2 from the COO− groups of CMC [4,5,44,46,47]. The last peak from DTG corresponded to the slow mass loss between 330–700 °C. However, the thermal reaction of the composite films occurred in a five-step process. The initial decomposition reason was the same as the control film at 85 °C. The second thermal reaction occurred in the temperature range of 150–260 °C, which reflects the volatilization of CFEO from the complex [48]. The third mass loss occurred between 260–330 °C. The fourth decomposition occurred at 330–400 °C, demonstrating that it was likely probably caused by some components from CFEO generates new bonds with CMC. The final weight loss tended to be slow between 420–700 °C. A comparison of the CFEO thermal reaction curves revealed that its thermal stability was enhanced through its combination with CMC.


(a)   (b)
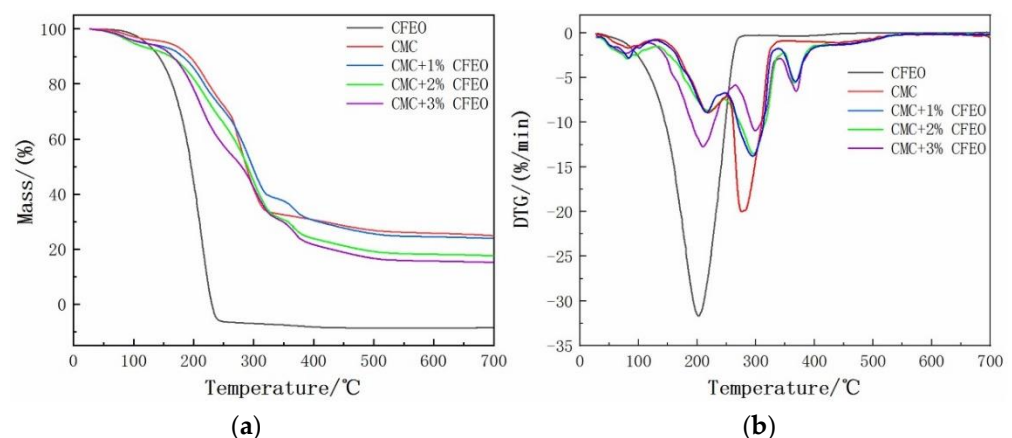
Figure 4. TGA (**a**) and DTG (**b**) curves for CFEO, CMC film, and blended CMC-CFEO films with various concentrations of CFEO.

3.6. DSC Analysis

The thermal properties of films are characterized by differential scanning calorimetric (DSC). Figure 5 and Table 4 show the endothermic changes and the thermal parameters, respectively. The endothermic peak at about 100–150 °C could be because the moisture was evaporated. After this, the endothermic peak at around 280 °C was associated to depolymerization and pyrolytic decomposition of CMC [49], which exhibited the peak melting temperature at 319.6 °C (Tm). In contrast with control film, the maximum melting temperature of the blended films shifted to the left, indicating that the CFEO can be used as a plasticizer to affect the mechanical properties of the films [50]. The Tm was larger than CMC film when the CFEO concentration was 2%. As the crystallinity of the composite films

increased, the EM and TS of the films increased, while the EB decreased. This was consistent with the results of mechanical properties research. With an increase in CFEO concentration, the crystallinity index (Xc) of the film decreased from 66.42 to 61.24, indicating that the film had the highest crystallinity after adding 1% CFEO. High crystallinity represented high thermal stability, proving that the addition of CFEO can improve the thermal stability of the film [51]. On the contrary, high concentrations of CFEO may destroy the crystal structure of the original material and have a negative impact on the mechanical properties of the film.
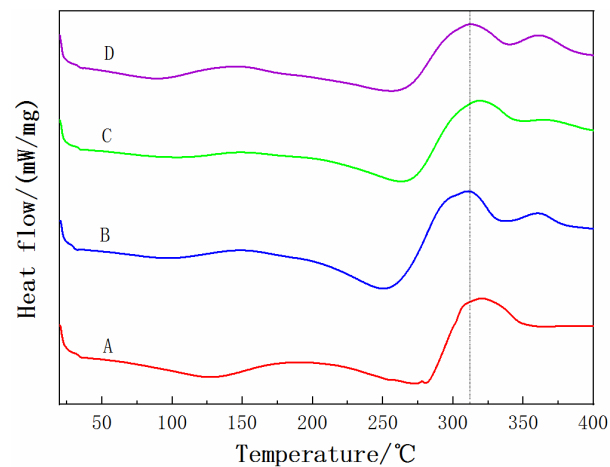
Figure 5. DSC thermograms of CMC film, and blended CMC-CFEO films with various concentrations of CFEO. A: Control film (CMC); B: CMC + 1% CFEO film; C: CMC + 2% CFEO film; D: CMC + 3% CFEO film.

Table 4. The melting temperature (Tm), enthalpy of melting (Hm) and crystallinity index (Xc) of CMC and blended CMC-CFEO films.

Film	Melting Temperature (Tm) (°C)	Enthalpy of Melting (Hm) (J/g)	Crystallinity Index (Xc) (%)
CMC	319.6	67.6	100
CMC + 1% CFEO	311.7	44.9	66.42
CMC + 2% CFEO	319.9	42.1	62.28
CMC + 3% CFEO	312.4	41.4	61.24

3.7. Mechanical Properties

Table 2 shows the mechanical characterization of the obtained films. The mechanical properties serve as important indices to evaluate the feasibility of food packaging materials. Figure 6 clearly shows the strain-stress curve of all films. The TS and EB were 1.75–5.25 MPa and 22.65%–63.16%, respectively. The value of EM was 3.96–18.06 MPa. As the CFEO concentration increased, the TS decreased. This result, which agrees with that reported by Sanchez-Gonzalez [52], occurred because a higher concentration of CFEO leads to weaker cross-linking interaction between polymers and CFEO [25]. Compared with that in the control film, the TS was obviously improved, indicating that the presence of CFEO had an effect on the TS and increased the flexibility. The EB presented the same trend, with the maximum level reached when the CFEO concentration was 1%. However, the EB of the composite film with CFEO concentrations of 2% and 3% was lower than the control film. This result occurred because the addition of CFEO led to the development of pores in the cross-section, which made the film matrix discontinuous and reduced the intermolecular and intramolecular forces [24,53]. During the film production, the loss of moisture content also affected the strain force of the composite films [54]. The EM of the blended films

increased significantly in comparison with the control film, indicating that the resistance to deformation of the films was enhanced. It seems that According to the experimental results, the best mechanical properties of the composite films were achieved after adding 1% CFEO.
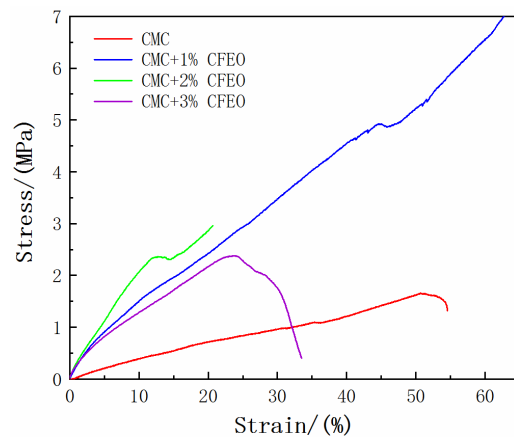
Figure 6. Stress-strain curves for CMC film and blended CMC-CFEO films with various concentrations of CFEO.

3.8. Microstructure Analysis

Figure 7 shows environmental scanning electron microscopy (ESEM) images of the film surfaces and cross-sections used to evaluate the form of CFEO in the films. The upper panels show the surface microstructure of the films, which exhibited prominent differences between the CMC film and the blended CMC-CFEO films. The CMC film had smooth surfaces without pores, resulting in continuous structures [24]. Although the blended CMC-CFEO films also had smooth surfaces, abundant pores and cavities also appeared as the amount of CFEO increased. A similar microstructure in chitosan–CMC films containing essential oil has been reported in previous research [55]. The increase in pores on the surface relative to the increase in CFEO concentration is attributed to coalescence of essential oil droplets. This phenomenon is clearly exhibited in the cross-section images in the lower panels in the figure, reflecting the lipid droplets embedded in the film matrix [56]. The number and diameter of the lipid droplets increased slightly as the CFEO concentration increased, which demonstrates the powerful aggregation force of CFEO in CMC [57].
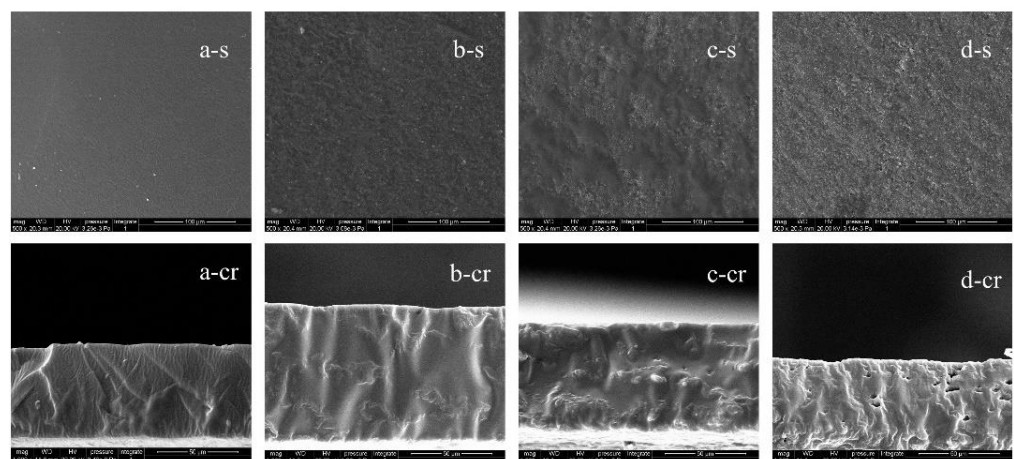
Figure 7. Surface (s; upper) (100 μm) and cross-section (cr; lower) (50 μm) microstructure images of CMC film and blended CMC–CFEO film: (**a**): control film (CMC); (**b**): CMC + 1% CFEO film; (**c**): CMC + 2% CFEO film; (**d**): CMC + 3% CFEO film.

3.9. Antimicrobial Activity Analysis

Table 5 shows the antimicrobial effects of CFEO and blended CMC-CFEO film on foodborne pathogens, which were analyzed by measuring the clear zone diameters [58]. In the bacterial strains tested, the CMC film had no bacteriostatic effect, and its inhibition diameter was zero. Although the CFEO and composite films showed good antibacterial effects toward *S. aureus*, that toward *E. coli* and *B. subtilis* was not obvious. This occurred because the inhibitory effect of essential oils on gram-positive bacteria is slightly stronger than that of gram-negative bacteria, which is related to the composition of essential oils, the antibacterial mechanism, and the structure of the gram-negative bacteria [59,60]. Gram-negative bacteria have an outer membrane on the surface, and the surface coverage of lipopolysaccharide restricts the penetration of essential oils, making the antibacterial effect insignificant [59]. However, not all essential oils exhibit the same behavior [61]. In this study, the antibacterial effect of CFEO was stronger toward gram-positive bacteria than gram-negative bacteria.

Table 5. Inhibitory zone diameters of CFEO and the CMC films incorporated with CFEO against *S. aureus*, *E. coli*, *B. subtilis*, and *P. citrinum*.

Experimental Group	*S. aureus* (mm)	*P. citrinum* (mm)	*E. coli* (mm)	*B. subtilis* (mm)
CMC	–	–	–	–
CFEO	15.1 ± 0.1 [a]	10.0 ± 0.1 [b]	6.0 [a]	8.8 ± 0.2 [a]
CMC + 1% CFEO	7.2 ± 0.3 [d]	8.8 ± 0.4 [c]	6.0 [a]	6.0 [b]
CMC + 2% CFEO	8.7 ± 0.4 [c]	13.3 ± 1.5 [b]	6.0 [a]	6.0 [b]
CMC + 3% CFEO	11.5 ± 0.7 [b]	19.5 ± 2.1 [a]	6.0 [a]	6.0 [b]

"–": no antimicrobial effect. The letters after the numbers in the same column are not the same, indicating that there is a significant ($p < 0.05$) difference.

Moreover, the inhibitory effect toward *S. aureus* on the composite film was lower than that found on CFEO alone. This result could be attributed to the partial loss of volatile compounds during the emulsion process and the slower diffusion rate of phenolic compounds into the agar [62]. Similarly, the CFEO yielded a clear inhibition zone for *P. citrinum* and exhibited good inhibitory effects toward food-borne fungi. The comparative results showed that the composite films presented a larger zone of inhibition for *P. citrinum*. Figure 8 shows the antimicrobial effect of all films. The composite films showed that the inhibition zone gradually widened when the CFEO concentration increased. In particular, 3% CFEO had the largest inhibition zone against the strains. Neither the addition of an emulsifier nor the film-formation process affected the antimicrobial effect of CFEO. Therefore, the present study proved that the CMC film incorporated with CFEO can be used as safe food packaging film.
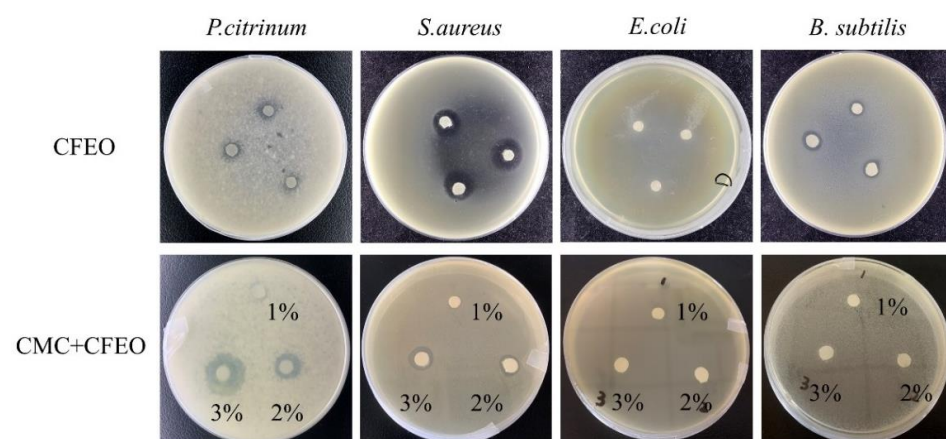
Figure 8. Comparison of inhibition zones in CFEO and composite films. The clear zone around the filter paper is the inhibition zone.

3.10. Weight Loss

Figure 9 shows the weight loss of Shine Muscat grapes during storage. Significant changes of weight loss could be seen on the 3rd day of storage. The weight loss of the control group and the CFEO group was significantly higher than the blended CMC-CFEO groups. On the 15th day, the weight loss of the control group was rapidly increased to 0.75%, which was evidently higher than other groups. On the 18th day, the weight loss of the CFEO group (0.92%) exceeded that of the control group. On the 18th day, the weight loss of CMC + 1% CFEO, CMC +2 %CFEO and CMC + 3% CFEO were 0.56%, 0.65%, and 0.68%, respectively. The comparative results showed that the composite groups achieved good performance of food preservation. The combination of a lower concentration of CFEO and CMC exhibited a good interaction. This was because CFEO had hydrophobic properties, which improved the moisture absorption property of CMC, thereby covering the surface of the fruit with a good hydrophobic barrier to reduce weight loss [15,63]. However, the combination of higher concentration of CFEO and CMC was not effective, maybe it was due to the large number of pores on the surface that allowed water vapor to enter. This conclusion was confirmed in the ESEM images.
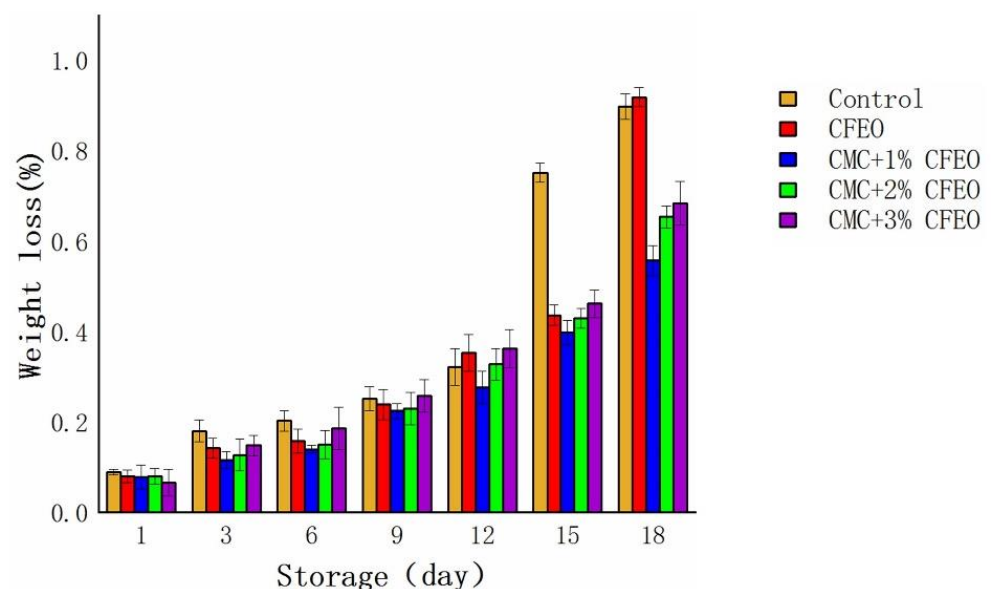
Figure 9. The effect of different treatment groups on weight loss of Shine Muscat grapes.

3.11. Decay Percentage

CFEO can inhibit the growth of fungi and its excellent antimicrobial activity can reduce the decay percentage of fruits. Figure 10 shows the decay percentage of Shine Muscat grapes during storage. It could be seen that in the first 12 days of storage, there was no fruit decay in the group of the blended CMC-CFEO. The decay in the control group and the CFEO group both appeared on the 3rd day and the decay percentage was 20%. From the 6th to the 18th, the decay percentage of the CFEO group was always higher than other groups, indicating that the pure CFEO cannot be coated on the surface of the fruit to achieve the preservation. As shown in Figure 11, with the increased of CFEO concentration, the fruit decay percentage of the blended CMC-CFEO continued to increase. This phenomenon verified the fact that 1% CFEO compound CMC had a good performance in reducing the decay of fruits. Table 6 shows the comparison of some recently studies and this work, which deals with natural extracts or essential oils in cellulose derivative films on food preservation. The comparison underlines the highlights of this work.
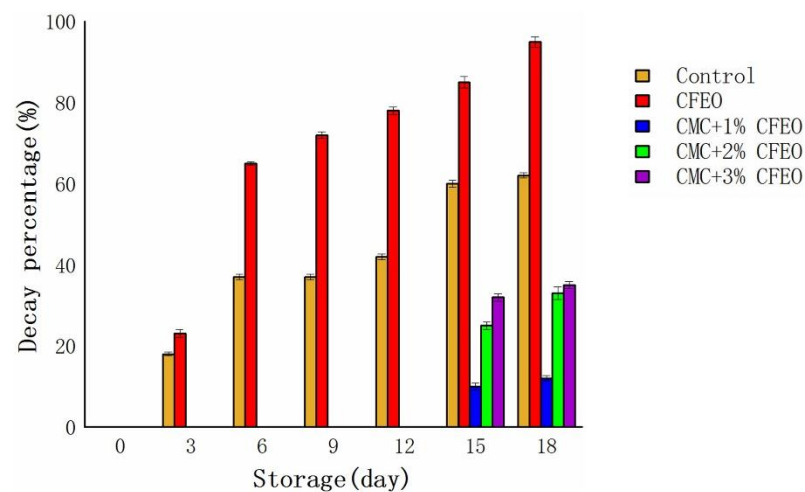
Figure 10. The effect of different treatment groups on decay percentage of Shine Muscat grapes.
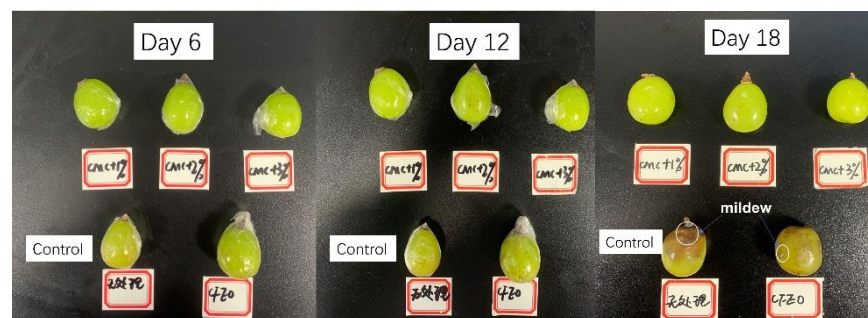

Figure 11. Appearance of Shine Muscat grapes coated with different treatment groups.

Table 6. Comparison of some recently studies dealing with natural extracts or essential oils in cellulose derivative films.

Natural Extracts	Polymer Matrix	Fresh Time	Storage Temperature	Application	Fungi	Ref.
CFEO	CMC	18 days	25 °C	Grapes	*P. citrinum*	This paper
ChNC/GSE	CMC	—	—	—	—	[64]
BEOs	CMC	—	—	—	*C. glabrata*	[33]
MSO	CMC/CH	12 days	4 °C	Strawberries	—	[26]
CEO	Chitosan/ZnO/Ag NPs	14 days	30 °C	Grapes	*C. albicans*	[20]

4. Conclusions

The addition of CFEO had a certain effect on CMC film. In comparison with control film, the transparency of the blended CFEO-CMC films decreased with an increase in CFEO concentration. The WS property indicated that the composite films had biodegradable properties. In addition, the concentration of CFEO directly affected the mechanical properties of the composite film. The CMC film mixed with 1% CFEO had the highest TS and EB, whereas a greater CFEO concentration decreased the flexibility. The total color difference increased with an increase in CFEO concentration, although the perceived transparency decreased. The combination of CFEO with CMC improved the thermal stability of the CFEO and slowed its volatilization rate. The cross-section of the composite films showed more holes, which increased in abundance with higher concentrations of CFEO. Moreover, the CMC films incorporated with CFEO showed good inhibitory effects toward *S. aureus* and *P. citrinum*. When 1% CFEO was mixed with CMC, the weight loss and decay percentage of Shine Muscat grapes were the lowest. The greater the concentration of CFEO, the worse the preservation effect. The results of this analysis indicate that CMC film combined with CFEO can be considered as an excellent food packaging material. Specifically, when used for food preservation and packaging, this material can reduce

the damage by foodborne pathogens and improve the food quality. In future research, the feasibility of this composite film for food preservation will be further evaluated in experiments on the basis of its physical and chemical indices.

Author Contributions: Conceptualization, L.M. and L.S.; Investigation, L.M.; Writing—original draft, L.M.; Project administration, K.Z.; Resources, Q.C.; Supervision, L.S.; Data curation, R.Z., X.S., and S.L. All authors have read and agreed to the published version of the manuscript.

Institutional Review Board Statement: Not applicable for studies not involving humans.

Informed Consent Statement: Not applicable for studies not involving humans.

Data Availability Statement: The data presented in this study are available in article.

Conflicts of Interest: The authors declare no conflict of interest.

References

1. Cha, D.S.; Chinnan, M.S. Biopolymer-based antimicrobial packaging: A review. *Crit. Rev. Food. Sci.* **2004**, *44*, 223–237. [CrossRef] [PubMed]
2. Suppakul, P.; Miltz, J.; Sonneveld, K.; Bigger, S.W. Active packaging technologies with an emphasis on antimicrobial packaging and its applications. *J. Food Sci.* **2003**, *68*, 408–420. [CrossRef]
3. Azarifar, M.; Ghanbarzadeh, B.; Khiabani, M.S.; Basti, A.A.; Abdulkhani, A. The effects of gelatin-CMC films incorporated with chitin nanofiber and Trachyspennum ammi essential oil on the shelf life characteristics of refrigerated raw beef. *Int. J. Food Microbiol.* **2020**, *318*. [CrossRef] [PubMed]
4. Su, J.-F.; Huang, Z.; Yuan, X.-Y.; Wang, X.-Y.; Li, M. Structure and properties of carboxymethyl cellulose/soy protein isolate blend edible films crosslinked by Maillard reactions. *Carbohyd. Polym.* **2010**, *79*, 145–153. [CrossRef]
5. Ma, X.; Chang, P.R.; Yu, J. Properties of biodegradable thermoplastic pea starch/carboxymethyl cellulose and pea starch/microcrystalline cellulose composites. *Carbohyd. Polym.* **2008**, *72*, 369–375. [CrossRef]
6. Salama, H.E.; Aziz, M.S.A.; Sabaa, M.W. Development of antibacterial carboxymethyl cellulose/chitosan biguanidine hydrochloride edible films activated with frankincense essential oil. *Int. J. Biol. Macromol.* **2019**, *139*, 1162–1167. [CrossRef]
7. Ghanbarzadeh, B.; Almasi, H. Physical properties of edible emulsified films based on carboxymethyl cellulose and oleic acid. *Int. J. Biol. Macromol.* **2011**, *48*, 44–49. [CrossRef]
8. Ghanbarzadeh, B.; Almasi, H.; Entezami, A.A. Improving the barrier and mechanical properties of corn starch-based edible films: Effect of citric acid and carboxymethyl cellulose. *Ind. Crop. Prod.* **2011**, *33*, 229–235. [CrossRef]
9. Ghanbarzadeh, B.; Almasi, H.; Entezami, A.A. Physical properties of edible modified starch/carboxymethyl cellulose films. *Innov. Food Sci. Emerg.* **2010**, *11*, 697–702. [CrossRef]
10. Holley, R.A.; Patel, D. Improvement in shelf-life and safety of perishable foods by plant essential oils and smoke antimicrobials. *Food Microbiol.* **2005**, *22*, 273–292. [CrossRef]
11. Matsumoto, H.; Ikoma, Y. Effect of postharvest temperature on the muscat flavor and aroma volatile content in the berries of 'Shine Muscat' (Vitis labruscana Baily × V. vinifera L.). *Postharvest Biol. Tec.* **2016**, *112*, 256–265. [CrossRef]
12. Lim, Y.-S.; Hassan, O.; Chang, T. First report of anthracnose of shine muscat caused by colletotrichum fructicola in Korea. *Mycobiology* **2020**, *48*, 75–79. [CrossRef] [PubMed]
13. Nakajima, I.; Endo, M.; Haji, T.; Moriguchi, T.; Yamamoto, T. Embryogenic callus induction and Agrobacterium-mediated genetic transformation of 'Shine Muscat' grape. *Plant Biotechnol.-NAR* **2020**, *37*, 185–194. [CrossRef] [PubMed]
14. Suehiro, Y.; Mochida, K.; Itamura, H.; Esumi, T. Skin browning and expression of PPO, STS, and CHS genes in the grape berries of 'Shine Muscat'. *J. Jpn. Soc. Hortic. Sci.* **2014**, *83*, 122–132. [CrossRef]
15. Dong, F.; Wang, X. Effects of carboxymethyl cellulose incorporated with garlic essential oil composite coatings for improving quality of strawberries. *Int. J. Biol. Macromol.* **2017**, *104*, 821–826. [CrossRef]
16. Servili, A.; Feliziani, E.; Romanazzi, G. Exposure to volatiles of essential oils alone or under hypobaric treatment to control postharvest gray mold of table grapes. *Postharvest Biol. Tec.* **2017**, *133*, 36–40. [CrossRef]
17. Abdollahi, A.; Hassani, A.; Ghosta, Y.; Bernousi, I.; Meshkatalsadat, M.H.; Shabani, R.; Ziaee, S.M. Evaluation of essential oils for maintaining postharvest quality of Thompson seedless table grape. *Nat. Prod. Res.* **2012**, *26*, 77–83. [CrossRef]
18. De Simone, N.; Pace, B.; Grieco, F.; Chimienti, M.; Tyibilika, V.; Santoro, V.; Capozzi, V.; Colelli, G.; Spano, G.; Russo, P. Botrytis cinerea and table grapes: A review of the main physical, chemical, and bio-based control treatments in post-harvest. *Foods* **2020**, *9*, 1138. [CrossRef]

19. Kumar, S.; Boro, J.C.; Ray, D.; Mukherjee, A.; Dutta, J. Bionanocomposite films of agar incorporated with ZnO nanoparticles as an active packaging material for shelf life extension of green grape. *Heliyon* **2019**, *5*, e01867. [CrossRef]
20. Motelica, L.; Ficai, D.; Ficai, A.; Trusca, R.-D.; Ilie, C.-I.; Oprea, O.-C.; Andronescu, E. Innovative antimicrobial chitosan/ZnO/Ag NPs/citronella essential oil nanocomposite-potential coating for grapes. *Foods (Basel Switz.)* **2020**, *9*, 1801. [CrossRef]
21. Aloui, H.; Khwaldia, K.; Sanchez-Gonzalez, L.; Muneret, L.; Jeandel, C.; Hamdi, M.; Desobry, S. Alginate coatings containing grapefruit essential oil or grapefruit seed extract for grapes preservation. *Int. J. Food. Sci. Tech.* **2014**, *49*, 952–959. [CrossRef]
22. Bakkali, F.; Averbeck, S.; Averbeck, D.; Waomar, M. Biological effects of essential oils—A review. *Food Chem. Toxicol.* **2008**, *46*, 446–475. [CrossRef] [PubMed]
23. Hyldgaard, M.; Mygind, T.; Meyer, R.L. Essential oils in food preservation: Mode of action, synergies, and interactions with food matrix components. *Front. Microbiol.* **2012**, *3*. [CrossRef] [PubMed]
24. Han, Y.; Yu, M.; Wang, L. Physical and antimicrobial properties of sodium alginate/carboxymethyl cellulose films incorporated with cinnamon essential oil. *Food Packag. Shelf Life* **2018**, *15*, 35–42. [CrossRef]
25. Dashipour, A.; Razavilar, V.; Hosseini, H.; Shojaee-Aliabadi, S.; German, J.B.; Ghanati, K.; Khakpour, M.; Khaksar, R. Antioxidant and antimicrobial carboxymethyl cellulose films containing Zataria multiflora essential oil. *Int. J. Biol. Macromol.* **2015**, *72*, 606–613. [CrossRef]
26. Shahbazi, Y. Application of carboxymethyl cellulose and chitosan coatings containing Mentha spicata essential oil in fresh strawberries. *Int. J. Biol. Macromol.* **2018**, *112*, 264–272. [CrossRef] [PubMed]
27. Shi, J.; Zhen, Y.; Zheng, R.-H. Proteome profiling of early seed development in Cunninghamia lanceolata (Lamb.) Hook. *J. Exp. Bot.* **2010**, *61*, 2367–2381. [CrossRef] [PubMed]
28. Yang, W.-D.; Liu, J.-S.; Li, H.-Y.; Zhang, X.-L.; Qi, Y.-Z. Inhibition of the growth of Alexandrium tamarense by Algicidal Substances in Chinese Fir (Cunninghamia lanceolata). *Bull. Environ. Contam. Toxicol.* **2009**, *83*, 537–541. [CrossRef]
29. Zhao, M.; Xiang, W.; Peng, C.; Tian, D. Simulating age-related changes in carbon storage and allocation in a Chinese fir plantation growing in southern China using the 3-PG model. *Forest Ecol. Manag.* **2009**, *257*, 1520–1531. [CrossRef]
30. Su, Y.-C.; Ho, C.-L.; Wang, E.I.C. Analysis of leaf essential oils from the indigenous five conifers of Taiwan. *Flavour Fragr. J.* **2006**, *21*, 447–452. [CrossRef]
31. Cheng, S.S.; Chang, H.T.; Chang, S.T.; Tsai, K.H.; Chen, W.J. Bioactivity of selected plant essential oils against the yellow fever mosquito Aedes aegypti larvae. *Bioresour. Technol.* **2003**, *89*, 99–102. [CrossRef]
32. Mohammadi, M.; Azizi, M.H.; Zoghi, A. Antimicrobial activity of carboxymethyl cellulose-gelatin film containing Dianthus barbatus essential oil against aflatoxin-producing molds. *Food Sci. Nutr.* **2020**, *8*, 1244–1253. [CrossRef] [PubMed]
33. Rincon, E.; Serrano, L.; Balu, A.M.; Aguilar, J.J.; Luque, R.; Garcia, A. Effect of bay leaves essential oil concentration on the properties of biodegradable carboxymethyl cellulose-based edible films. *Materials* **2019**, *12*, 2356. [CrossRef] [PubMed]
34. Poaty, B.; Lahlah, J.; Porqueres, F.; Bouafif, H. Composition, antimicrobial and antioxidant activities of seven essential oils from the North American boreal forest. *World J. Microb. Biot.* **2015**, *31*, 907–919. [CrossRef] [PubMed]
35. Ye, Z.; Lin, W.; Chen, W.; Yu, X. Chemical components and antimicrobial activity of essential oils in Cunninghamia lanceolata heartwood. *J. Appl. Ecol.* **2005**, *16*, 2394–2398.
36. Huang, L.H.; Qin, T.F.; Tatsuro, O. Studies on preparations and analysis of essential oil from Chinese fir. *J. For. Res.* **2004**, *15*, 80–82.
37. Feng, S.L.; Xin, C.; Liu, X.J.; Feng, Y.W. Study on chemical constituents of the essential oil from the root of Cunninghamia lanceolata. *Flavour Fragr. Cosmet.* **2000**, *2*, 391–392.
38. Chang, S.T.; Cheng, S.S.; Wang, S.Y. Antitermitic activity of essential oils and components from Taiwania (Taiwania cryptomerioides). *J. Chem. Ecol.* **2001**, *27*, 717–724. [CrossRef]
39. Abdollahi, M.; Damirchi, S.; Shafafi, M.; Rezaei, M.; Ariaii, P. Carboxymethyl cellulose-agar biocomposite film activated with summer savory essential oil as an antimicrobial agent. *Int. J. Biol. Macromol.* **2019**, *126*, 561–568. [CrossRef]
40. Shojaee-Aliabadi, S.; Hosseini, H.; Mohammadifar, M.A.; Mohammadi, A.; Ghasemlou, M.; Ojagh, S.M.; Hosseini, S.M.; Khaksar, R. Characterization of antioxidant-antimicrobial kappa-carrageenan films containing Satureja hortensis essential oil. *Int. J. Biol. Macromol.* **2013**, *52*, 116–124. [CrossRef]
41. Mohsenabadi, N.; Rajaei, A.; Tabatabaei, M.; Mohsenifar, A. Physical and antimicrobial properties of starch-carboxy methyl cellulose film containing rosemary essential oils encapsulated in chitosan nanogel. *Int. J. Biol. Macromol.* **2018**, *112*, 148–155. [CrossRef] [PubMed]
42. Ruan, C.; Zhang, Y.; Wang, J.; Sun, Y.; Gao, X.; Xiong, G.; Liang, J. Preparation and antioxidant activity of sodium alginate and carboxymethyl cellulose edible films with epigallocatechin gallate. *Int. J. Biol. Macromol.* **2019**, *134*, 1038–1044. [CrossRef] [PubMed]
43. Mir, S.; Yasin, T.; Siddiqi, H.M.; Murtaza, G. Thermal, rheological, mechanical and morphological behavior of high density polyethylene and carboxymethyl cellulose blend. *J. Polym. Environ.* **2017**, *25*, 1011–1020. [CrossRef]
44. Arnon-Rips, H.; Sabag, A.; Tepper-Bamnolker, P.; Chalupovich, D.; Levi-Kalisman, Y.; Eshel, D.; Porat, R.; Poverenov, E. Effective suppression of potato tuber sprouting using polysaccharide-based emulsified films for prolonged release of citral. *Food Hydrocoll.* **2020**, *103*. [CrossRef]
45. Mirzaei-Mohkam, A.; Garavand, F.; Dehnad, D.; Keramat, J.; Nasirpour, A. Physical, mechanical, thermal and structural characteristics of nanoencapsulated vitamin E loaded carboxymethyl cellulose films. *Prog. Org. Coat.* **2020**, *138*. [CrossRef]
46. Teotia, A. Modification of carboxymethyl cellulose through oxidation. *Carbohyd. Polym.* **2012**, *87*, 457–460. [CrossRef]

47. Rajeh, A.; Morsi, M.A.; Elashmawi, I.S. Enhancement of spectroscopic, thermal, electrical and morphological properties of polyethylene oxide/carboxymethyl cellulose blends: Combined FT-IR/DFT. *Vacuum* **2019**, *159*, 430–440. [CrossRef]

48. Yuan, C.; Thomas, D.S.; Hook, J.M.; Qin, G.; Qi, K.; Zhao, J. Molecular encapsulation of Eucalyptus staigeriana essential oil by forming inclusion complexes with hydroxypropyl-beta-cyclodextrin. *Food Bioprocess Tech.* **2019**, *12*, 1264–1272. [CrossRef]

49. Liu, T.; Wang, J.; Chi, F.; Tan, Z.; Liu, L. Development and characterization of novel active chitosan films containing fennel and peppermint essential oils. *Coatings* **2020**, *10*, 936. [CrossRef]

50. Qin, Y.; Li, W.; Liu, D.; Yuan, M.; Li, L. Development of active packaging film made from poly (lactic acid) incorporated essential oil. *Prog. Org. Coat.* **2017**, *103*, 76–82. [CrossRef]

51. Grande Tovar, C.D.; Ivan Castro, J.; Valencia Llano, C.H.; Navia Porras, D.P.; Delgado Ospina, J.; Valencia Zapata, M.E.; Herminsul Mina Hernandez, J.; Chaur, M.N. Synthesis, characterization, and histological evaluation of chitosan-ruta graveolens essential oil films. *Molecules* **2020**, *25*, 1688. [CrossRef] [PubMed]

52. Sanchez-Gonzalez, L.; Chafer, M.; Chiralt, A.; Gonzalez-Martinez, C. Physical properties of edible chitosan films containing bergamot essential oil and their inhibitory action on Penicillium italicum. *Carbohyd. Polym.* **2010**, *82*, 277–283. [CrossRef]

53. Moradi, M.; Tajik, H.; Rohani, S.M.R.; Oromiehie, A.R.; Malekinejad, H.; Aliakbarlu, J.; Hadian, M. Characterization of antioxidant chitosan film incorporated with Zataria multiflora Boiss essential oil and grape seed extract. *LWT-food Sci. Technol.* **2012**, *46*, 477–484. [CrossRef]

54. Hosseini, M.H.; Razavi, S.H.; Mousavi, M.A. Antimicrobial, physical and mechanical properties of chitosan-based films incorporated with thyme, clove and cinnamon essential oils. *J. Food Process. Preserv.* **2009**, *33*, 727–743. [CrossRef]

55. Noshirvani, N.; Ghanbarzadeh, B.; Gardrat, C.; Rezaei, M.R.; Hashemi, M.; Le Coz, C.; Coma, V. Cinnamon and ginger essential oils to improve antifungal, physical and mechanical properties of chitosan-carboxymethyl cellulose films. *Food Hydrocolloid.* **2017**, *70*, 36–45. [CrossRef]

56. Sanchez-Gonzalez, L.; Vargas, M.; Gonzalez-Martinez, C.; Chiralt, A.; Chafer, M. Characterization of edible films based on hydroxypropylmethylcellulose and tea tree essential oil. *Food Hydrocolloid.* **2009**, *23*, 2102–2109. [CrossRef]

57. Sanchez-Gonzalez, L.; Gonzalez-Martinez, C.; Chiralt, A.; Chafer, M. Physical and antimicrobial properties of chitosan-tea tree essential oil composite films. *J. Food Eng.* **2010**, *98*, 443–452. [CrossRef]

58. Jouki, M.; Yazdi, F.T.; Mortazavi, S.A.; Koocheki, A. Quince seed mucilage films incorporated with oregano essential oil: Physical, thermal, barrier, antioxidant and antibacterial properties. *Food Hydrocolloid.* **2014**, *36*, 9–19. [CrossRef]

59. Burt, S. Essential oils: Their antibacterial properties and potential applications in foods—A review. *Int. J. Food Microbiol.* **2004**, *94*, 223–253. [CrossRef]

60. Dorman, H.J.; Deans, S.G. Antimicrobial agents from plants: Antibacterial activity of plant volatile oils. *J. Appl. Microbiol.* **2000**, *88*, 308–316. [CrossRef]

61. Wilkinson, J.M.; Hipwell, M.; Ryan, T.; Cavanagh, H.M.A. Bioactivity of backhousia citriodora: Antibacterial and antifungal activity. *J. Agr. Food Chem.* **2003**, *51*, 76–81. [CrossRef] [PubMed]

62. Benavides, S.; Villalobos-Carvajal, R.; Reyes, J.E. Physical, mechanical and antibacterial properties of alginate film: Effect of the crosslinking degree and oregano essential oil concentration. *J. Food Eng.* **2012**, *110*, 232–239. [CrossRef]

63. Sanchez-Gonzalez, L.; Pastor, C.; Vargas, M.; Chiralt, A.; Gonzalez-Martinez, C.; Chafer, M. Effect of hydroxypropyl methylcellulose and chitosan coatings with and without bergamot essential oil on quality and safety of cold-stored grapes. *Postharvest Biol. Tec.* **2011**, *60*, 57–63. [CrossRef]

64. Oun, A.A.; Rhim, J.-W. Preparation of multifunctional carboxymethyl cellulose-based films incorporated with chitin nanocrystal and grapefruit seed extract. *Int. J. Biol. Macromol.* **2020**, *152*, 1038–1046. [CrossRef]